



Bowl-in-bowl encapsulation of corannulene by heteroatom-bridged nanobelts

Xia Li^{a,1}, Yandie Liu^{a,1}, Zhenglin Du^a, Qiangsheng Zhang^b, Qing Chen^a, Jialin Xie^{b,c,*}, Kelong Zhu^{a,*}

^aSchool of Chemistry, Sun Yat-Sen University, Guangzhou 510275, China

^bHainan Provincial Key Laboratory of Fine Chem, School of Chemistry and Chemical Engineering, Hainan University, Haikou 570228, China

^cOne Health Institute, Hainan University, Haikou 570228, China

ARTICLE INFO

Article history:

Received 27 March 2024

Revised 9 July 2024

Accepted 15 July 2024

Available online 15 July 2024

Keywords:

Nanobelt

Corannulene

Host-guest chemistry

Molecular recognition

Bowl-in-bowl

ABSTRACT

Nanobelts are a rapidly developing family of macrocycles with appealing features. However, their host-guest chemistry is currently limited to the recognition of fullerenes via $\pi-\pi$ interactions. Herein, we report two heteroatom-bridged [8]cyclophoxathiin nanobelts ([8]CP-Me and [8]CP) encapsulate corannulene (Cora) to form bowl-in-bowl supramolecular structures stabilized mainly through CH- π interactions in solid-state. The convex surface of corannulene is oriented towards the cavity due to geometry complementarity. The complex Cora@[8]CP exhibits a unique 2:2 capsule-like structure in crystal packing, in which corannulene adopts a concave-to-concave assembling fashion. This work enriches the molecular recognition of nanobelts and demonstrates that CH- π interactions can act as the main driving force for nanobelts host-guest complexes.

© 2025 Published by Elsevier B.V. on behalf of Chinese Chemical Society and Institute of Materia Medica, Chinese Academy of Medical Sciences.

Corannulene (Cora) (Fig. 1), a bowl-shaped aromatic electron acceptor, can be considered as a fragment of fullerene C₆₀ [1]. It possesses a dynamic skeleton exhibiting a bowl-to-bowl inversion at room temperature [2]. Its edge hydrogen atoms are suitable for CH- π interactions [3,4], making it suitable for studying intricate host-guest systems that rely on interactions involving dispersion forces [4–15]. However, its non-polar and bowl-shaped structure causes it challenging to be efficiently recognized and complexed by supramolecular hosts. Consequently, driven by the hydrophobic effect, Cora has been mostly trapped in cyclophanes [5,6] or metal-organic cages [10–15] featuring structural complementarity.

Non-covalent interactions and structural complementarity are vital to supramolecular chemistry and utilized in virtually every field of science and engineering. Despite being a relatively weak non-covalent interaction controlled by dispersion forces [16], CH- π interactions play important roles in not only protein folding [17] but also crystal packing [18]. In addition, facilitated by hydrophobic effect or structural complementarity, the CH- π interactions, normally subsidiary in host-guest recognition, can act as the sole force

for encapsulating non-spherical guests within nanoring cavities of cycloparaphenylenes (CPPs) and their derivatives [4,19–22]. For example, Isobe and co-workers demonstrated that a π -expansion CPP could wrap corannulene to form a bowl-in-tube complex driven exclusively by CH- π interactions [4].

Nanobelts, a class of rigid double-stranded macrocycles, have advanced remarkably [23–25]. However, the research on their host-guest recognition is still limited, mainly focusing on those nanobelts-fullerene host-guest complexes stabilized by $\pi-\pi$ interactions [26–30]. Recently, we have developed a series of heteroatom-bridged nanobelts [29–31], in which the bowl-shaped [8]cyclophoxathiins ([8]CP and [8]CP-Me) can encapsulate fullerenes (*i.e.*, C₆₀, C₇₀, and PC₆₁BM) with strong affinity via $\pi-\pi$ interactions (Fig. 1a) [29,30]. Based on these results, we hypothesized that [8]CP and [8]CP-Me could also interact with Cora to form bowl-in-bowl complexes stabilized by CH- π bonds, despite Cora having a slightly larger diameter and lower structural complementarity relative to C₆₀.

The nanobelt [8]CP-Me was prepared according to our previous work [30]. The association behavior of [8]CP-Me with Cora was first confirmed by ¹H NMR of their equimolar solution in CDCl₃. As shown in Fig. 2, the signals of the proton from Cora underwent an up-field chemical shift by 0.126 ppm compared to the free Cora. As for [8]CP-Me, the protons of the upper rim (H_a and H_b) slightly

* Corresponding authors.

E-mail addresses: xiejialin@hainanu.edu.cn (J. Xie), zhukelong@mail.sysu.edu.cn (K. Zhu).

¹ These authors contributed equally to this work.

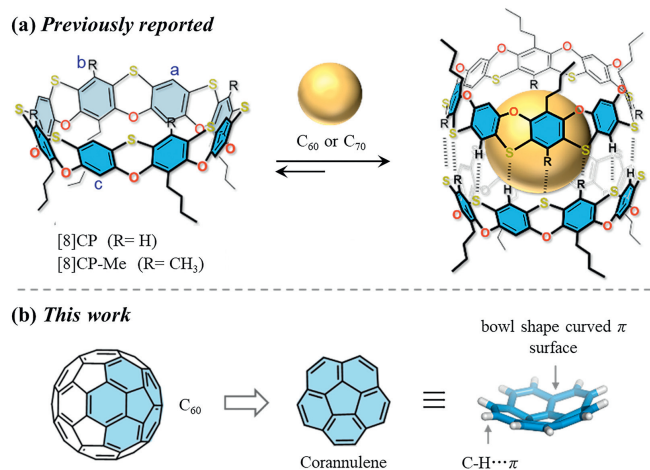


Fig. 1. (a) Previously reported two bowl-shaped nanobelts [8]cyclophoxathiins ([8]CP and [8]CP-Me) could encapsulate C₆₀ or C₇₀ to form hydrogen-bonded capsules. (b) Possible interactions between corannulene and nanobelts.

shifted to the down-field, yet the lower rim protons (H_c and butyl group protons) shifted to the up-field. These observations support the encapsulation of Cora inside the bowl-shaped cavity, shielded by the surrounding aromatic walls. Subsequently, ¹H NMR titration was performed to determine the association constants for the complex formed. With successive additions of Cora, continuous chemical shift changes for protons from both components were observed, demonstrating a fast complexation kinetics between Cora and [8]CP-Me within the NMR time scale. Combined with the 1:1 stoichiometric binding model given by Job's plot analysis (Figs. S2 and S3 in Supporting information), the association constant

(K_a) was determined to be 98 ± 0.6 L/mol ($\Delta G = -11.4$ kJ/mol) [32], which is consistent with our hypothesis that the decreased structural complementarity of Cora results in a weaker binding affinity with cyclophoxathiin nanobelts comparing to fullerene C₆₀ [30].

The structure and binding mode of this complex were finally determined by X-ray crystallographic analysis of suitable crystals obtained by diffusing methyl *tert*-butyl ether into a mixture of [8]CP-Me and Cora in CHCl₃ (Table S1 in Supporting information). The results revealed that [8]CP-Me tends to be ellipsoidal and adopts a 1:1 stoichiometric binding model. The convex surface of Cora is oriented towards the cavity due to shape complementarity. Interestingly, each crystal unit cell contains two Cora-[8]CP-Me complexes, in which Cora is bound to the cavity with different modes (Fig. 3). With a tilting angle of about 60°, Cora can π - π stack with the phenyl sidewall of [8]CP-Me at centroid-to-centroid distances of 3.92 Å and 4.03 Å, respectively (Fig. 3a). In addition, the average distance between the Cora protons and the phenyl plane of [8]CP-Me is 3.16 Å, supporting the presence of CH- π interactions. Similarly, in the other complex within the same cell unit, Cora is suspended inside the cavity of the nanobelt at a smaller tilting angle (~30°) with CH- π bonds (averaged distance is 3.11 Å) as the main driven force (Fig. 3b).

Based on the binding mode between [8]CP-Me and Cora, we expected the nanobelt [8]CP would have a different association behavior with Cora, since the previous researches revealed that [8]CP could self-assembly into dimeric capsules in the presence of guest [29,30]. Fig. 4 depicts the ¹H NMR spectrum of an equimolar mixture of [8]CP-Me and Cora in C₂D₂Cl₄ (TCE-*d*₂) and shows the anticipated chemical shift changes following the encapsulation of Cora in the cavity of the nanobelt. However, ¹H NMR titration experiments revealed that all signals broadened as the amount of guests increased, with the most pronounced changes of the upper

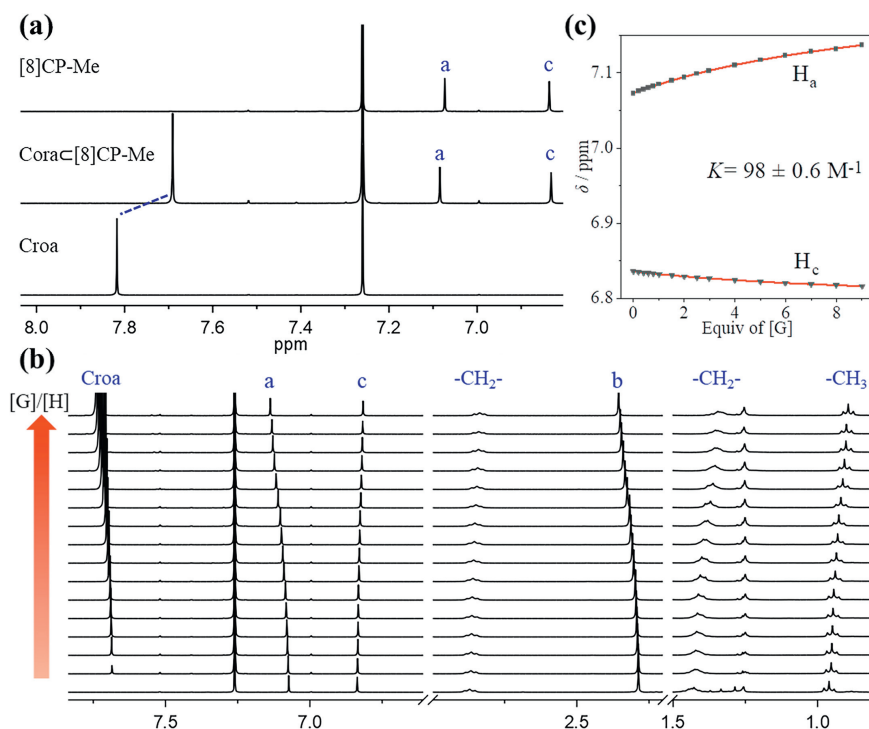


Fig. 2. Association behavior of [8]CP-Me with Cora monitored by ¹H NMR (400 MHz, CDCl₃, 298 K): (a) Partial ¹H NMR spectra of free [8]CP-Me, [8]CP-Me with 1.0 equiv. Cora, and free Cora (1.00 mmol/L). (b) Stacked ¹H NMR spectra of [8]CP-Me with increasing amounts of Cora. (c) Non-linear fitting curve for protons H_a and H_c of [8]CP-Me. NMR peak assignment was referenced to Fig. 1a.

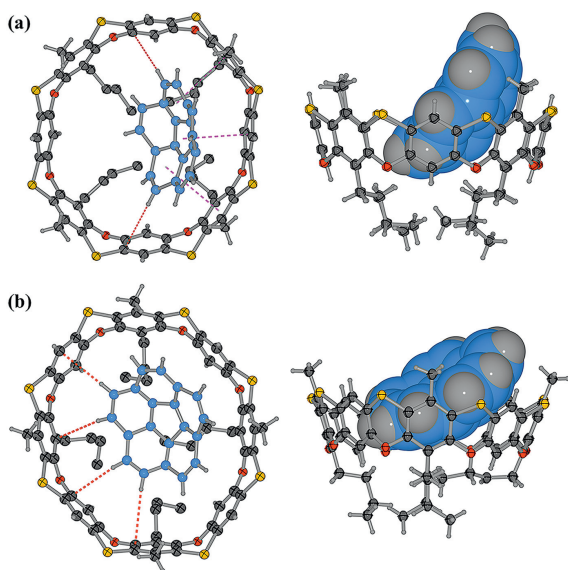


Fig. 3. Single-crystal X-ray structure of the complex CoraC[8]CP-Me. (a) and (b) illustrate the two different types of host-guest complexes within one asymmetric unit cell. The $\pi-\pi$ and $\text{CH}\cdots\pi$ interactions are highlighted in purple and red dash lines, respectively.

rim protons (H_a and H_b). This suggests an equilibrium state that is close to coalescence [33], which was confirmed by X-ray crystallographic analysis (see below). Based on the Job's plot method (Figs. S8 and S9 in Supporting information), a nonlinear regression analysis of the NMR titration data with 1:1 binding stoichiometry af-

forded an association constant value of $94 \pm 0.4 \text{ L/mol}$ ($\Delta G = -11.3 \text{ kJ/mol}$) [32].

The suitable single crystals of complex CoraC[8]CP for X-ray crystallography were obtained by slow diffusion *n*-hexane into a mixture of [8]CP and Cora in TCE, which have several distinct features compared to CoraC[8]CP-Me (Fig. 5 and Table S4 in Supporting information). Firstly, [8]CP adopts a regular octagon shape, while Cora guest is suspended slightly tilted inside the cavity, and its ArH protons are in close contact with the aromatic walls of [8]CP, thus establishing multiple $\text{CH}-\pi$ bonds as the main driving force to stabilize this complex with an average bond length of 3.16 \AA , while the $\pi-\pi$ interaction between the host and guest only had less contribution. This result was further supported by the IGMH (independent gradient method based on Hirshfeld partition) calculations (Fig. 6a) and Hirshfeld surfaces analysis (Fig. 6b, Figs. S15–S17 in Supporting information), which provide qualitative and quantitative description of the involvement of supramolecular interactions within the CoraC[8]CP complex. Moreover, similar to the previous results observed for CoraC[8]CP-Me, the [8]CP tends to form two slightly different dimeric capsule-like structures in the crystal packing mode depending on the tilting angle of Cora (Figs. 5a and b). The larger tilting angle (Fig. 5c left) forms a tightly packed capsule structure with a cyclic seam of weak $\text{C}-\text{H}\cdots\text{S}$ hydrogen bonds ($d_{\text{S}\cdots\text{H}} = 3.15 \text{ \AA}$, Table S3 in Supporting information) on the equatorial window, whereas the smaller tilting angle causes the two hosts to be staggered with each other and lose some hydrogen bonds (Fig. 5c right and Table S2 in Supporting information). Most importantly, the crystal packing not only leads to a unique 2:2 capsule-in-capsule topology, but the Cora also forms an unusual concave-to-concave assembly in a capsule-shape fashion [9,10], which usually undergoes convex-to-concave unidirectional columnar stacking in solid-state [1,4].

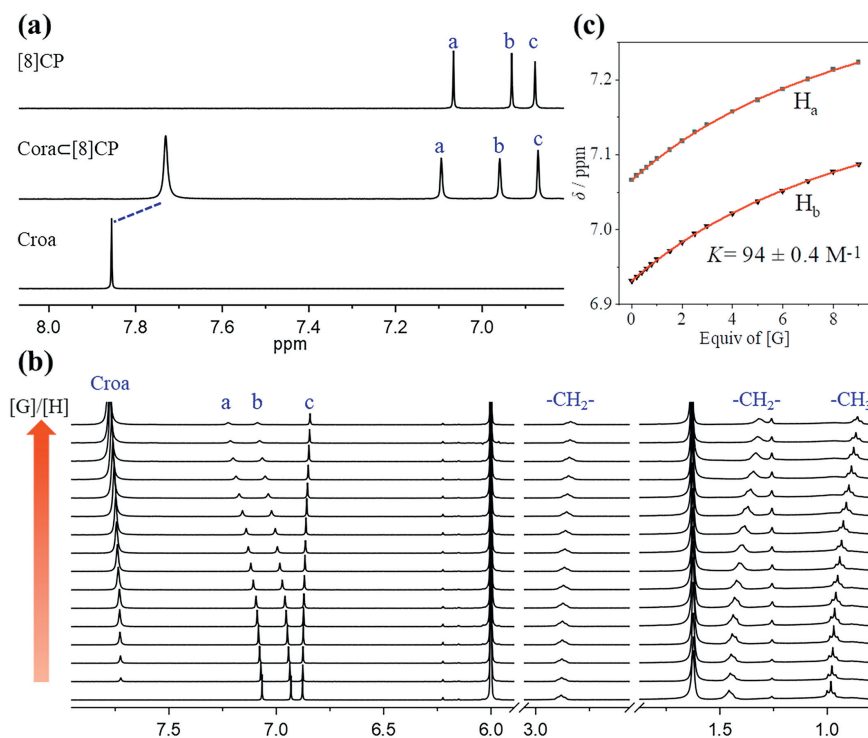


Fig. 4. Association behavior of [8]CP with Cora monitored by ^1H NMR (400 MHz, $\text{TCE}-d_2$, 298 K): (a) Partial ^1H NMR spectra of free [8]CP, [8]CP with 1.0 equiv. Cora, and free Cora (1.00 mmol/L). (b) Stacked ^1H NMR spectra of [8]CP with increasing amounts of Cora. (c) Non-linear fitting curve for protons H_a and H_b of [8]CP. NMR peak assignment was referenced to Fig. 1a.

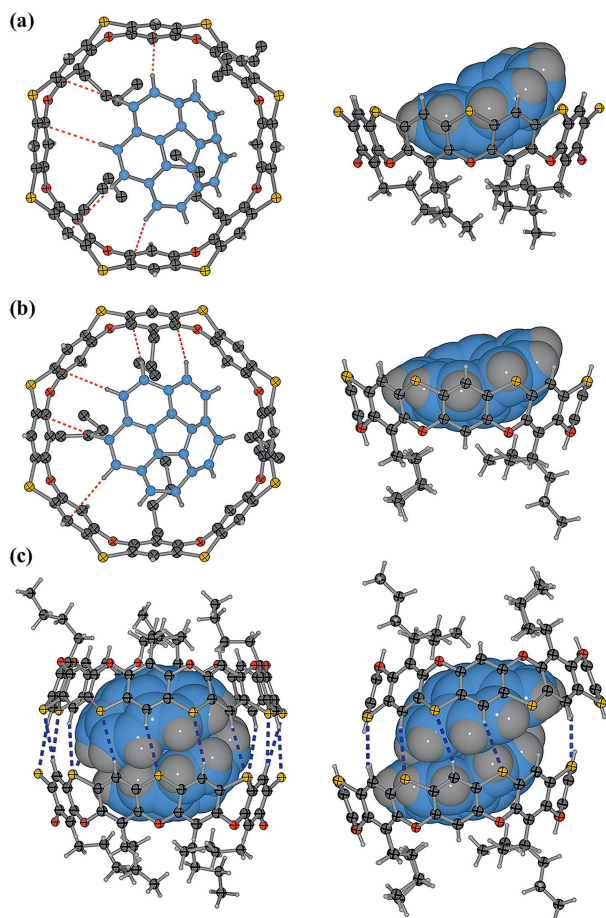


Fig. 5. Single-crystal X-ray structure of the complex Corac[8]CP. (a) and (b) depict the two distinct types of host-guest complexes within a single asymmetric unit cell, with a hemisphere displayed. (c) shows the complete structures of these complexes. CH... π interactions and C-H...S hydrogen bonds are highlighted in red and blue dash lines, respectively.

In conclusion, we have investigated the host-guest chemistry of bowl-shaped nanobelts [8]cyclophenoxythiins ([8]CP-Me and [8]CP) and corannulene in both solution and solid-state, and obtained the bowl-in-bowl complex stabilized by multiple CH- π bonds for nanobelts. Due to shape complementarity, the convex surface of corannulene orients toward the cavity and is inclined to bind inside the cavity. Although structural similarity for these two nanobelts, [8]CP tends to form dimeric capsules, resulting in the complex Corac[8]CP assembled mainly by CH- π bonds. In crystal packing, it can further form a unique 2:2 capsule structure, and corannulene also forms an unusual concave-to-concave assembly in a capsule-shaped fashion. These results further expand the host-guest recognition capability of such heteroatom-bridged nanobelts.

Declaration of competing interest

The authors declare that they have no known competing financial interests or personal relationships that could have appeared to influence the work reported in this paper.

CRediT authorship contribution statement

Xia Li: Writing – original draft, Investigation. **Yandie Liu:** Investigation. **Zhenglin Du:** Investigation. **Qiangsheng Zhang:** Investigation. **Qing Chen:** Investigation. **Jialin Xie:** Writing – review & editing. **Kelong Zhu:** Writing – review & editing, Writing – original draft, Supervision, Funding acquisition, Conceptualization.

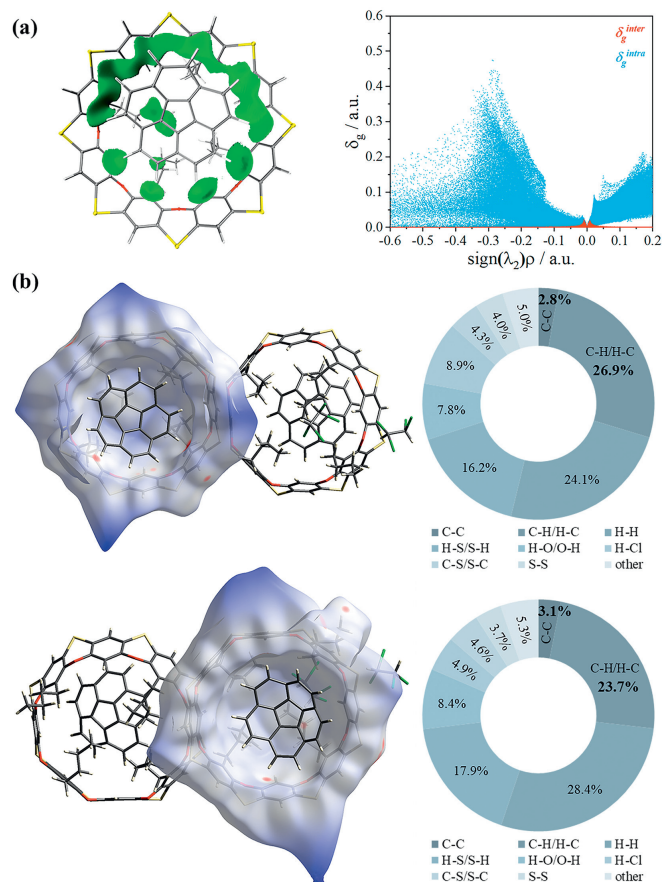


Fig. 6. IGMH calculations (a) and Hirshfeld surfaces analyses (b) of crystalline Corac[8]CP.

Acknowledgments

We thank the National Natural Science Foundation of China (No. 22171295), the Fundamental Research Funds for the Central Universities (No. 23xkjc006), Guangzhou Science and Technology Programme (No. 2024A04J6423), Innovative Fund for Scientific and Technological Personnel of Hainan Province (No. KJRC2023D34) for financial support.

Supplementary materials

Supplementary material associated with this article can be found, in the online version, at doi:10.1016/j.ccl.2024.110249.

References

- [1] Y.T. Wu, J.S. Siegel, Chem. Rev. 106 (2006) 4843–4867.
- [2] L.T. Scott, M.M. Hashemi, M.S. Bratcher, J. Am. Chem. Soc. 114 (1992) 1920–1921.
- [3] X. Li, F.Y. Kang, M. Inagaki, Small 12 (2016) 3206–3223.
- [4] T. Matsuno, M. Fujita, K. Fukunaga, S. Sato, H. Isobe, Nat. Commun. 9 (2018) 3779.
- [5] M. Juríček, N.L. Strutt, J.C. Barnes, et al., Nat. Chem. 6 (2014) 222–228.
- [6] A.A. Kroeger, A. Karton, Org. Chem. Front. 8 (2021) 4408–4418.
- [7] H. Joshi, S. Sreejith, R. Dey, M.C. Stuparu, RSC Adv. 6 (2016) 110001–110110.
- [8] J. Kang, D. Miyajima, T. Mori, et al., Science 347 (2015) 646–651.
- [9] Y.D. Yang, X.L. Chen, J.L. Sessler, H.Y. Gong, J. Am. Chem. Soc. 143 (2021) 2315–2324.
- [10] N. Kishi, Z. Li, Y. Sei, et al., Chem. Eur. J. 19 (2013) 6313–6320.
- [11] B.M. Schmidt, T. Osuga, T. Sawada, M. Hoshino, M. Fujita, Angew. Chem. Int. Ed. 55 (2016) 1561–1564.
- [12] Q.J. Fan, Y.J. Lin, F.E. Hahn, G.X. Jin, Dalton Trans. 47 (2018) 2240–2246.
- [13] S. Ibáñez, E. Peris, Angew. Chem. Int. Ed. 59 (2020) 6860–6865.
- [14] Y. Yang, T.K. Ronson, Z.F. Lu, et al., Nat. Commun. 12 (2021) 4079.

- [15] S. Hasegawa, A. Baksi, B. Chen, G. Clever, *Org. Mater.* 4 (2022) 222–227.
- [16] M. Nishio, *Phys. Chem. Chem. Phys.* 13 (2011) 13873–13900.
- [17] M. Nishio, Y. Umezawa, J. Fantini, M.S. Weiss, P. Chakrabarti, *Phys. Chem. Chem. Phys.* 16 (2014) 12648–12683.
- [18] M. Nishio, *CrystEngComm* 6 (2004) 130–158.
- [19] S. Adachi, M. Shibasaki, N. Kumagai, *Nat. Commun.* 10 (2019) 3820.
- [20] T. Matsuno, K. Fukunaga, S. Sato, H. Isobe, *Angew. Chem. Int. Ed.* 58 (2019) 12170–12174.
- [21] H. Kwon, C.J. Bruns, *Nano Res.* 15 (2022) 5545–5555.
- [22] P.D. Sala, C. Talotta, T. Caruso, et al., *J. Org. Chem.* 82 (2017) 9885–9889.
- [23] H. Chen, Q. Miao, *J. Phys. Org. Chem.* 33 (2020) e4145.
- [24] T.H. Shi, M.X. Wang, *CCS Chem.* 3 (2021) 916–931.
- [25] Y.M. Li, H. Kono, T. Maekawa, et al., *Acc. Mater. Res.* 2 (2021) 681–691.
- [26] X. Lu, T.Y. Gopalakrishna, Y. Han, et al., *J. Am. Chem. Soc.* 141 (2019) 5934–5941.
- [27] Z. Xia, S.H. Pun, H. Chen, Q. Miao, *Angew. Chem. Int. Ed.* 60 (2021) 10311–10318.
- [28] J. Pfeuffer-Rooschüz, L. Schmid, A. Prescimone, K. Tiefenbacher, *JACS Au* 1 (2021) 1885–1891.
- [29] J.L. Xie, X. Li, S.H. Wang, et al., *Nat. Commun.* 11 (2020) 3348.
- [30] J.L. Xie, X. Li, Z.L. Du, Y.D. Liu, K.L. Zhu, *CCS Chem.* 5 (2023) 958–970.
- [31] S.H. Wang, J. Yuan, J.L. Xie, et al., *Angew. Chem. Int. Ed.* 60 (2021) 18443–18447.
- [32] P. Thordarson, *Chem. Soc. Rev.* 40 (2011) 1305–1323.
- [33] C. Peinador, E. Pía, V. Blanco, M.D. García, J.M. Quintela, *Org. Lett.* 12 (2010) 1380–1383.